Journal of Sound and Vibration ▮ (▮▮▮▮) ▮▮▮–▮▮▮

Contents lists available at ScienceDirect

Journal of Sound and Vibration

journal homepage: www.elsevier.com/locate/jsvi

Intensity of oscillation of spark-generated bubbles

Silvano Buogo [a], Karel Vokurka [b,*]

[a] CNR – Istituto di Acustica e Sensoristica "O.M. Corbino", via Fosso del Cavaliere 100, 00133 Roma, Italy
[b] Physics Department, Technical University of Liberec, Studentská 2, 461 17 Liberec, Czech Republic

ARTICLE INFO

Article history:
Received 14 December 2009
Received in revised form
9 April 2010
Accepted 23 April 2010
Handling Editor: L. Huang

ABSTRACT

In this paper, a new measure of bubble oscillation intensity is introduced, defined as a non-dimensional peak pressure in the first bubble pulse. An iterative method for determining the bubble size and bubble oscillation intensity from a record of the acoustic pressure wave emitted by an oscillating bubble is proposed. Using this procedure the sizes and intensities are determined for a set of pressure records obtained in recent experiments with spark-generated bubbles. It can be seen that in these experiments the bubble sizes, as defined by the first maximum bubble radius, R_{M1}, ranged from 12.8 to 56.4 mm, and the bubble oscillation intensities, as defined by the non-dimensional peak pressure in the first bubble pulse, p_{zp1}, ranged from 14.3 to 174. Data obtained in the experiments are compared with data computed in a theoretical model and it is shown that there are differences between the theory and experiment. These differences are attributed to energy losses from the real bubbles not taken into account in the theoretical model.

1. Introduction

Bubbles that oscillate in liquids may either perform useful work, as in ultrasonic cleaners [1,2], or act harmfully, as for example with cavitation in hydraulic machinery [1,2]. For both these reasons oscillating bubbles have long been subjects of intensive research.

A freely oscillating (pulsating) spherical bubble is basically described by its size and intensity of oscillations [3]. It is the intensity of bubble oscillations first of all (but not exclusively) that plays an important role in all processes associated with bubbles. In Ref. [3] amplitude has been suggested as a suitable measure of bubble oscillation intensity (the amplitude is defined as the ratio of maximum and equilibrium bubble radii, see Eq. (2) below) and a method for determining the amplitude from experimental data, based on scaling functions, has been described. A disadvantage of that method is that in this way the amplitude is not determined directly from measured data but indirectly via the scaling functions, and the scaling functions have been derived only in a theoretical form so far.

In this paper, we want to introduce another measure of bubble oscillation intensity, which is the non-dimensional peak pressure in the first bubble pulse. An advantage of this measure is that it can be computed from the measured data directly and thus it can be used to compare different experiments without making use of scaling functions. Nevertheless, the previous intensity measure, the amplitude, retains its importance in theoretical computations and can be determined from the non-dimensional peak pressure via the scaling functions as previously noted. In such a way it is also possible to compare experiments with theory.

* Corresponding author.
E-mail addresses: silvano.buogo@idasc.cnr.it (S. Buogo), karel.vokurka@tul.cz (K. Vokurka).

0022-460X/$ - see front matter © 2010 Elsevier Ltd. All rights reserved.
doi:10.1016/j.jsv.2010.04.030

The method suggested here is based on evaluating acoustic pressures radiated by oscillating bubbles. By analyzing the pressure records both the bubble oscillation intensities and bubble sizes could be determined. The method is illustrated by evaluating a large set of pressure records measured recently in experiments with spark-generated bubbles.

However, before starting analyzing the experimental data it seems useful to review the concept of the bubble oscillation intensity in a theoretical framework first. This will be done in the next section. Then an experimental setup used to capture high-speed films of the bubbles and to measure the pressure records will be briefly described and examples of the measured data will be shown in Section 3. In Section 4 an iterative procedure allowing determining both bubble size and bubble oscillation intensity from acoustic pressure waves radiated by oscillating bubbles will be introduced. Using the iterative procedure, a scatter plot of intensity vs. size values (the so-called 'bubble map') for the experimental spark bubbles will be given. Finally, experimental and theoretical time plots of bubble radius and of radiated pressure waves will be compared in Section 5.

2. Bubble oscillation intensity

To introduce the concept of bubble oscillation intensity a model of the so-called gas bubble will be used first. The intensity measure developed for gas bubbles will be then applied to spark generated bubbles.

Let us assume a spherical bubble, being in rest in an extended liquid (far from boundaries). The bubble has a radius R_0 and is filled with gas. Let the ambient (hydrostatic) pressure at the place of the bubble be p_∞ and the pressure in the liquid at the bubble wall be P_0. Finally, let the liquid temperature be Θ_∞. In the following, the ambient pressure p_∞ and temperature Θ_∞ will be assumed to be known, as they usually can be determined in experiments easily.

At time t_0 let the bubble be excited to start free oscillations (pulsations) by using one of the three basic excitations methods [3]. Even if the real excitation method does play an important role in further bubble life, here we shall only assume that at a time $t_1 \geq t_0$ the oscillating spherical bubble attains its first maximum radius $R_{M1} > R_0$. Let us further assume that the pressure and temperature fields in the bubble interior be spatially homogeneous at the time t_1 and their values be equal to $P_{m1} < P_0$ and Θ_{m1}, respectively. As the bubble wall motion is always slow in the vicinity of the maximum volume, to assume the two fields to be spatially homogeneous does not seem to be too far from reality.

It will be also assumed that we know the physical properties of both liquid and gas (density, velocity of sound, viscosity, etc.). Then, for a given combination of liquid, gas in the bubble interior, ambient pressure p_∞, and temperature Θ_∞, the bubble state at the time t_1 is fully determined by the values of R_{M1}, P_{m1}, and Θ_{m1}. After inserting these values into equations defining a suitable bubble model we should be able to determine, at least in theory, the bubble behavior at any further moment $t \geq t_1$. Although in a more simple form (based on a number of further simplifying assumptions) this task has already been solved a long time ago, an exhaustive description, in which more complex forms of bubble motions are considered, is still missing. Even if great efforts have been devoted to compare theory with experiments, this task has not been satisfactorily solved yet even in the case of the simplest oscillatory motions. However, the aim of this paper is not to fill this gap entirely, but rather to narrow it using the concept of the bubble oscillation intensity.

Of the three parameters mentioned above, namely R_{M1}, P_{m1}, and Θ_{m1}, attention will be paid to R_{M1} and P_{m1} only. Even if Θ_{m1} is also of great importance, it will be omitted from further discussion simply because at present time, according to our knowledge, there is no direct method enabling to determine the temperature in the gas Θ_{m1} experimentally. Thus, unfortunately, one can only speculate on what might be the real value of this parameter in a real experiment. In the following discussion the two remaining parameters, R_{M1} and P_{m1}, shall be interpreted as the measures of the bubble size and intensity of oscillations.

In theoretical works the equilibrium radius R_0 can be used to describe the bubble size. However, it is not an easy task to determine R_0 experimentally. In most experiments it is much simpler to determine the first maximum radius R_{M1}. This can be done, for example, by using a high-speed photography, or by evaluating pressure waves radiated by the oscillating bubbles. In Section 5 we shall discuss this second method of evaluating the experimental data.

The magnitude of R_0 (or R_{M1}) is decisive for taking into account influences of the surface tension, viscosity, heat conduction and gravity. To simplify the discussion, in this paper it shall be assumed that the bubble size is such that all these effects may be considered to be negligible. Bubbles of this size then obey scaling laws [3] and have been denoted as scaling bubbles accordingly. For scaling bubbles it holds that $P_0 = p_\infty$ and this relation can also be used to interpret the meaning of the equilibrium radius R_0 in those cases where the ambient pressure p_∞ is constant (see Eq. (A.2) in the Appendix).

After the oscillating bubble attains its maximum volume at a time t_1, it enters a compression phase. The achieved rate of gas compression inside the bubble depends on the mutual relation of P_{m1} and p_∞. This ratio will be denoted by an asterisk, i.e.

$$P^*_{m1} = \frac{P_{m1}}{p_\infty}. \tag{1}$$

The parameter P^*_{m1} can be used as a measure of the bubble oscillation intensity in theoretical computations. In this case the intensity of oscillations is indirectly proportional to P^*_{m1}. The smaller the non-dimensional pressure P^*_{m1}, the higher is the bubble oscillation intensity.

Please cite this article as: S. Buogo, & K. Vokurka, Intensity of oscillation of spark-generated bubbles, *Journal of Sound and Vibration* (2010), doi:10.1016/j.jsv.2010.04.030

Another suitable measure of the bubble oscillation intensity is a ratio of the first maximum radius R_{M1} to equilibrium radius R_0:

$$A_1 = \frac{R_{M1}}{R_0}. \tag{2}$$

This ratio has been denoted as the amplitude of the first bubble oscillation [3].

It can be easily shown that under the simplifying assumptions mentioned above for the scaling bubbles there is a simple relation between the two measures defined by Eqs. (1) and (2), namely

$$A_1 = (P^*_{m1})^{-1/3\gamma}. \tag{3}$$

Here γ is the ratio of specific heats of the gas inside the bubble. Thus, the two theoretical intensity measures are equivalent and if one is known, the other can easily be calculated from Eq. (3). Let us note that real value of γ cannot be determined from experimental data easily and thus its value used in theoretical computations is more or less speculative. A brief discussion concerning the value of γ can also be found, e.g., in Ref. [3].

Both the intensity measures introduced so far, P^*_{m1} and A_1, have their origin in theoretical bubble models. In Ref. [3] several possible ways are shown how to determine these intensity measures from experimental data. In the following, a new measure of bubble oscillation intensity will be introduced, which can be determined from experimental data more directly.

To illustrate the concept of bubble oscillation intensity, examples of theoretical variations of the bubble radius R with time t have been computed for four different values of the amplitude A_1. These variations are shown in Fig. 1a. The amplitudes selected for this purpose (A_1=1.25–2.00) correspond to weak nonlinear bubble oscillation intensities. The maximum bubble radii R_{M1} range from 25 to 40 mm, which is well within the range of the maximum radii of experimental bubbles discussed in Sections 4 and 5.

The plots of bubble radius vs. time $R(t)$ have been computed using a bubble model described in the Appendix. The liquid, ambient pressure p_∞, ratio γ, and bubble initial radius R_0 have been selected to allow an easy comparison with experimental data discussed in Sections 5 and 6. Bubbles of this size are assumed to fall within the range of scaling bubbles and this assumption makes interpretation of the results much easier.

Fig. 1a displays only small portions of the radius vs. time history. These portions correspond to a time interval (t_1, t_2), where t_1 and t_2 are the times when the bubble attains its first (R_{M1}) and second (R_{M2}) maximum volumes. To ease the comparison of different curves, the plots have been mutually shifted so that all bubbles attain their first minimum volumes (R=R_{m1}) at the same time, and such time is used as the time-scale origin (t=0) in this figure.

The range of amplitudes A_1 used to compute $R(t)$ has been selected to allow an easy comparison of the individual curves. However, as it will be shown in Section 5, the range of real oscillation intensities is much larger and the majority of experimental bubbles studied here actually oscillate with higher intensities.

In Fig. 1a the bubble oscillating with an amplitude A_1=1.25 can be considered to perform weakly nonlinear oscillations. As it can be seen, in this case the variation of radius R with time t departs only slightly from a damped harmonic motion. However, with increasing A_1, $R(t)$ starts deviating from harmonic motion very rapidly. It can be also seen that the larger the amplitude A_1, the smaller the minimum radius R_{m1}.

The interval between time t_1, when the bubble attains its first maximum radius R_{M1}, and the time when the bubble attains its first minimum radius R_{m1}, represents the time of the first bubble compression, T_{c1}, and we shall use it later to determine the bubble radius R_{M1}.

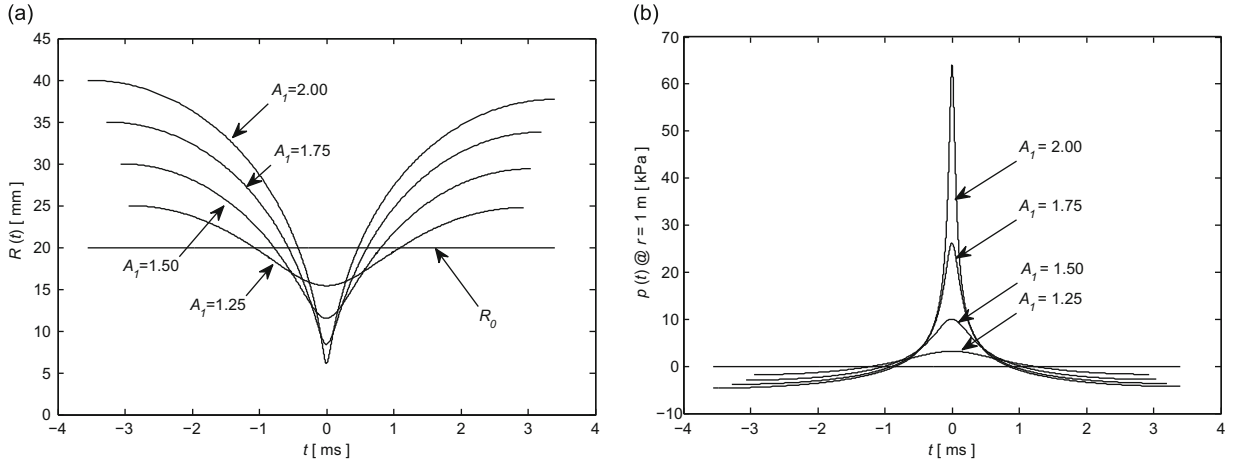

Fig. 1. (a) Computed time plots of bubble radius $R(t)$ for different amplitudes of oscillations A_1. (b) Computed time plots of radiated acoustic pressures $p(t)$ for different amplitudes of oscillation A_1.

Please cite this article as: S. Buogo, & K. Vokurka, Intensity of oscillation of spark-generated bubbles, *Journal of Sound and Vibration* (2010), doi:10.1016/j.jsv.2010.04.030

As the bubble oscillates it also radiates acoustic pressure waves into the surrounding liquid: a pulsating spherical bubble is in fact an excellent zero-order acoustic radiator. Examples of the radiated pressure waves computed for different bubble oscillation amplitudes A_1 are shown in Fig. 1b.

The acoustic pressure vs. time $p(t)$ have been computed using the bubble model described in the Appendix. The oscillation amplitudes A_1, initial radius R_0, ambient pressure p_∞, liquid and gas have been selected to be the same as in Fig. 1a.

The acoustic pressure waves have been computed at a nominal distance of $r=1$ m from the bubble center. Again, only portions of the pressure vs. time plots are displayed in Fig. 1b. The selected portions correspond to the same time interval (t_1 and t_2). Similarly, the plots have been shifted so that they attain their first peak values p_{p1} at the same time, which was set to be the time-scale origin ($t=0$).

Also note that for a relatively small amplitude $A_1=1.25$ the pressure vs. time history $p(t)$ departs only partially from a damped harmonic function. However, for larger amplitudes A_1 the radiated waves quickly take the shape of pressure pulses (called in this case the first bubble pulses). It should be noted that the peak pressure in the first bubble pulse, p_{p1}, is extremely sensitive to the value of the amplitude A_1 because p_{p1} can be determined experimentally, then it can be used as a convenient measure of bubble oscillation intensity in experimental works.

In underwater acoustics it is customary to characterize all sources by their emitted acoustic pressure measured at a nominal distance of 1 m [4]. However, in bubble research such a description would be satisfactory only if all bubbles were of the same size and oscillating under the same ambient pressure p_∞. In real life this is not the case and thus a more suitable description of the bubble as an acoustic radiator is done by using a non-dimensional peak pressure in the first bubble pulse p_{zp1} defined as

$$p_{zp1} = \frac{p_{p1}}{p_\infty}\,\frac{r}{R_{M1}}. \tag{4}$$

Let us remark that by multiplying the peak pressure p_{p1} with r this pressure is recalculated to a nominal distance $r=1$ m and by dividing it by R_{M1} it is recalculated for a nominal bubble size $R_{M1}=1$ m. By dividing this result with p_∞ we obtain finally a non-dimensional number.

In this paper, this non-dimensional peak pressure in the first bubble pulse is suggested to be a new measure of bubble oscillation intensity. In this case, by inserting experimental data into Eq. (4) we obtain a simple non-dimensional number describing the bubble oscillation intensity irrespective of the actual bubble size R_{M1} and distance r, at which the peak pressure p_{p1} has been measured.

The new measure of bubble oscillation intensity, p_{zp1}, is suitable when dealing with experimental pressure records first of all. However, we often need to interpret the data also by using the intensity measure derived from a theoretical model, i.e. A_1. Finding a satisfactory link between experimental data and a theoretical model is not a simple task (see, for example, the discussion in Ref. [3]). However, as a first approximation a functional dependence between p_{zp1} and A_1 can be computed using a theoretical model. The variation of A_1 with p_{zp1} computed with the bubble model described in the Appendix is given in Fig. 2.

Using Fig. 2, one can easily express the intensities of bubble oscillations shown in Fig. 1a and b using the new intensity measure. Thus, if the amplitude is $A_1=1.25$, the corresponding non-dimensional peak pressure is $p_{zp1}=1.02$, if $A_1=1.5$, then

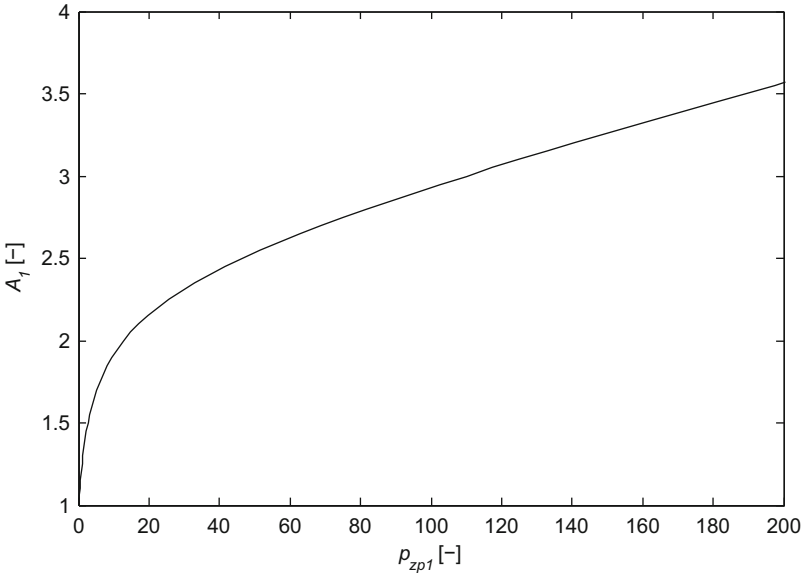

Fig. 2. Functional dependence between the non-dimensional peak pressure in the first bubble pulse p_{zp1} and amplitude of the first oscillation A_1.

Please cite this article as: S. Buogo, & K. Vokurka, Intensity of oscillation of spark-generated bubbles, *Journal of Sound and Vibration* (2010), doi:10.1016/j.jsv.2010.04.030

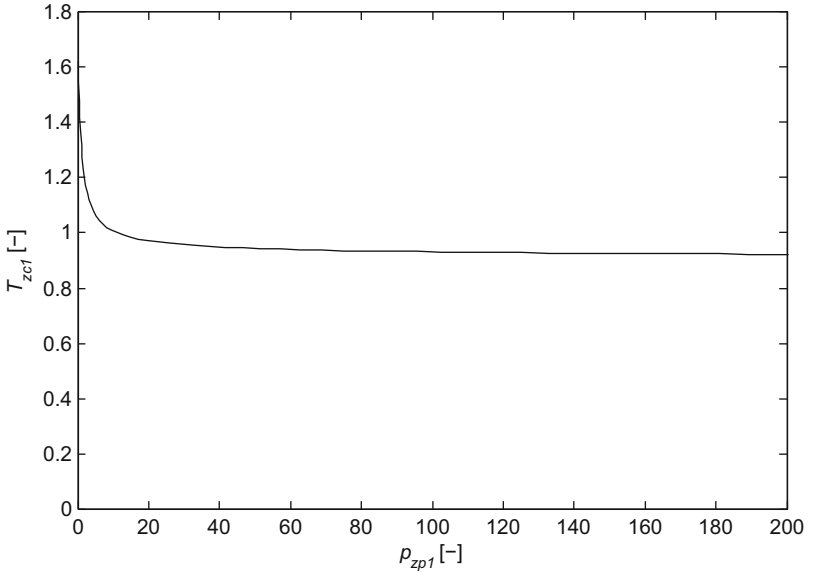

Fig. 3. Variation of the first non-dimensional compression time T_{zc1} with the non-dimensional peak pressure in the first bubble pulse p_{zp1}.

$p_{zp1}=2.7$, if $A_1=1.75$, then $p_{zp1}=6$ and finally if $A_1=2$, then $p_{zp1}=12.8$. We shall show later in Section 4, the intensities with which oscillate the spark generated bubbles are much higher.

As it can be seen in Figs. 1a and b, at a time t_1, when the bubble attains its maximum radius R_{M1}, it also radiates an acoustic pressure having a maximum negative (trough) value. When the bubble is compressed to the minimum radius R_{m1}, it radiates a positive peak pressure p_{p1}. By denoting t_{p1} the time when the positive peak is radiated, then the first compression time of the bubble equals $T_{c1}=t_{p1}-t_1$ (note that for simplicity the propagation time between the bubble wall and the point r in the liquid is not considered in this discussion).

The time of the first bubble compression T_{c1} can be conveniently used to estimate R_{M1} from pressure records obtained experimentally. For this purpose it is useful to introduce a non-dimensional compression time T_{zc1}

$$T_{zc1}=\frac{T_{c1}}{R_{M1}\sqrt{\rho_\infty/p_\infty}}. \tag{5}$$

As it can be seen in Figs. 1a and b, T_{c1} depends both on bubble size and on bubble oscillation intensity. To obtain a scaling function the dependence of T_{c1} on R_{M1} can be easily removed by dividing T_{c1} with R_{M1} as it is done in Eq. (5). The dependence of T_{c1} on p_{zp1} is more involved. Unfortunately, at present time this variation of T_{c1} vs. p_{zp1} has not been determined experimentally yet. Thus, as a first approximation, it is possible to compute the variation of T_{zc1} with p_{zp1} using the bubble model described in the Appendix. The variation thus determined is shown in Fig. 3. It can be seen that for $p_{zp1}>50$ the non-dimensional time of bubble compression is almost independent of p_{zp1}.

In Section 6 we shall apply the concepts introduced here to determine the bubble sizes and oscillation intensities in the case of experimental bubbles.

3. Experimental setup

Freely oscillating bubbles were generated in a laboratory water tank having dimensions 6 m × 4 m × 5.5 m using spark discharges. The experimental setup is schematically shown in Fig. 4.

The sparks were initiated between two electrodes (the sparker) made of tungsten wires of diameter 1–1.3 mm. The sparker was submerged in water at a depth of 2.5 m and about 1.2 m away from the nearest tank wall. The electrodes were connected to a capacitor bank, whose capacitance could be varied in steps. The capacitor bank was charged from a high voltage source, and an air-gap switch was used to trigger the discharge through the sparker.

Two configurations of the capacitor bank and high voltage source have been used. In the first case the total capacity could be varied in 40 μF steps from 40 to 360 μF and the charging voltage could be varied continuously from 2 to 2.6 kV. In the second case the bank capacity could be varied in steps of 16 μF from 16 to 160 μF and the charging voltage was 4 kV.

A limited number of high-speed camera records have been taken with a framing rate ranging from 2800 to 3000 frames/s. However, the main interest of this work was to study the acoustic pressure waves radiated by oscillating bubbles. These waves were recorded using two types of broadband hydrophones. The first hydrophone was Reson type TC 4034 with a nominal usable range from 1 Hz to 470 kHz and receiving sensitivity of −217.2 dB re 1 V/μPa. The second hydrophone was Reson type TC 4038 with a nominal usable range from 10 to 800 kHz and receiving sensitivity of −235.1 dB re 1 V/μPa. The hydrophones

Please cite this article as: S. Buogo, & K. Vokurka, Intensity of oscillation of spark-generated bubbles, *Journal of Sound and Vibration* (2010), doi:10.1016/j.jsv.2010.04.030

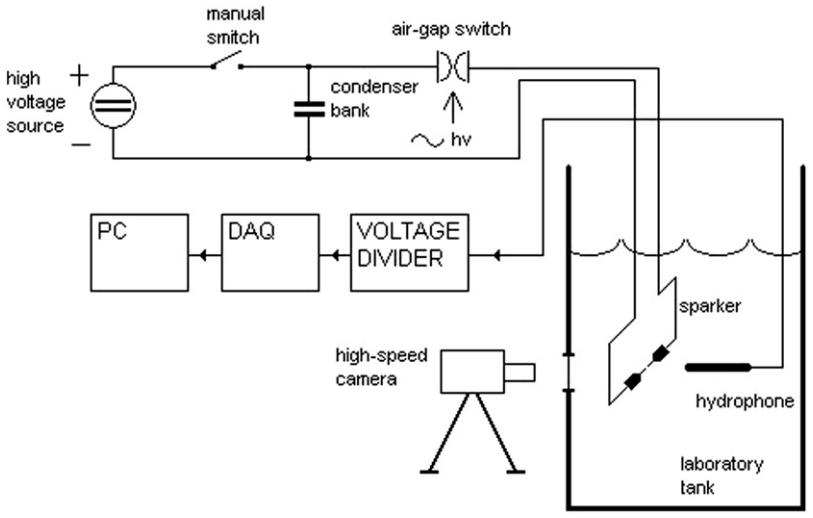

Fig. 4. Experimental setup for generating spark bubbles and recording their shape and radiated acoustic waves.

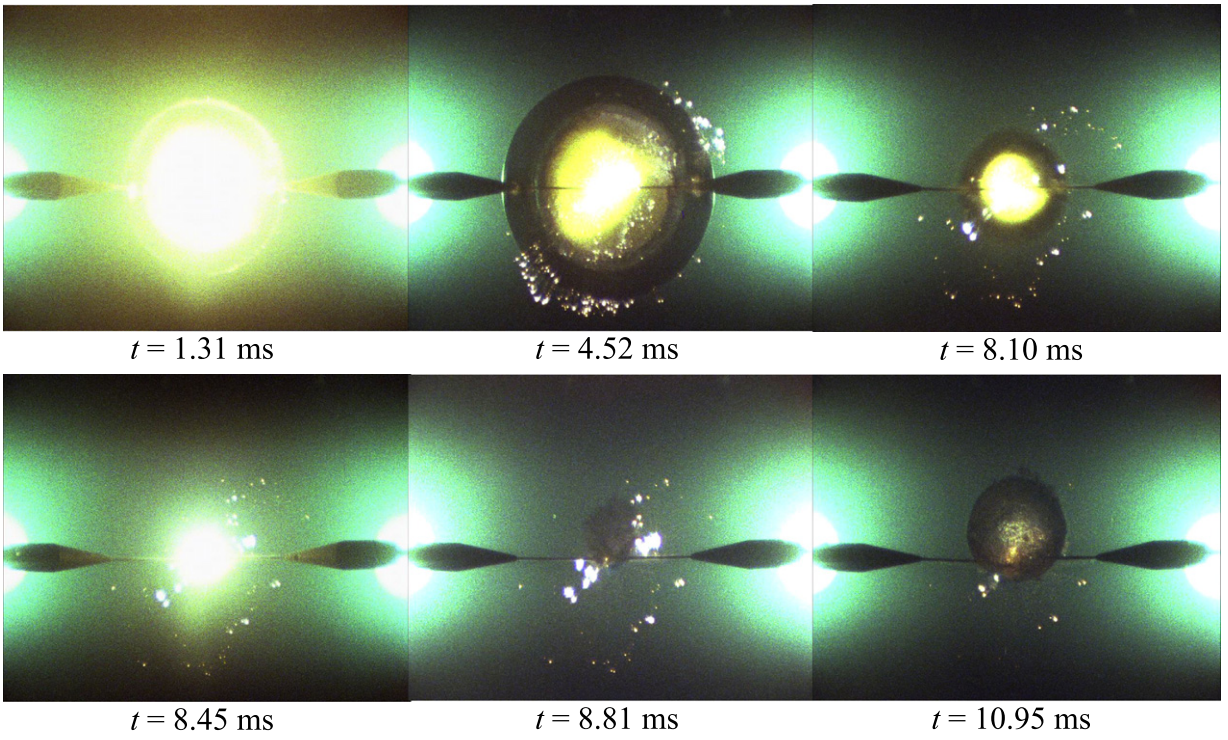

Fig. 5. Selected frames from a film record of the spark generated bubble (R_{M1} = 51.5 mm, p_{zp1} = 70.3, A_1 = 2.7156). Light spots at the frame's sides are due to illuminating lamps.

were positioned at distances r from the bubble center ranging from 0.1 to 2 m. The hydrophones were connected via voltage dividers to a digital acquisition board (National Instruments type NI 6115) having a resolution of 12 bits and sampling frequency 10 MHz. The length of each record was set to 20 ms.

Altogether 10 films have been taken in the experiments. Examples of several frames from one film corresponding to different times are given in Fig. 5.

In Fig. 5 the first frame corresponds to time when the intensive light generated by electric discharge has faded enough, so that the bubble starts to be visible. The second frame shows the bubble near its first maximum radius. The third and fourth frame show the bubble successively at the final stages of the compression, the fifth frame is the first view available after the bubble passed through the minimum volume and finally the sixth frame shows the bubble early after passing the

Please cite this article as: S. Buogo, & K. Vokurka, Intensity of oscillation of spark-generated bubbles, *Journal of Sound and Vibration* (2010), doi:10.1016/j.jsv.2010.04.030

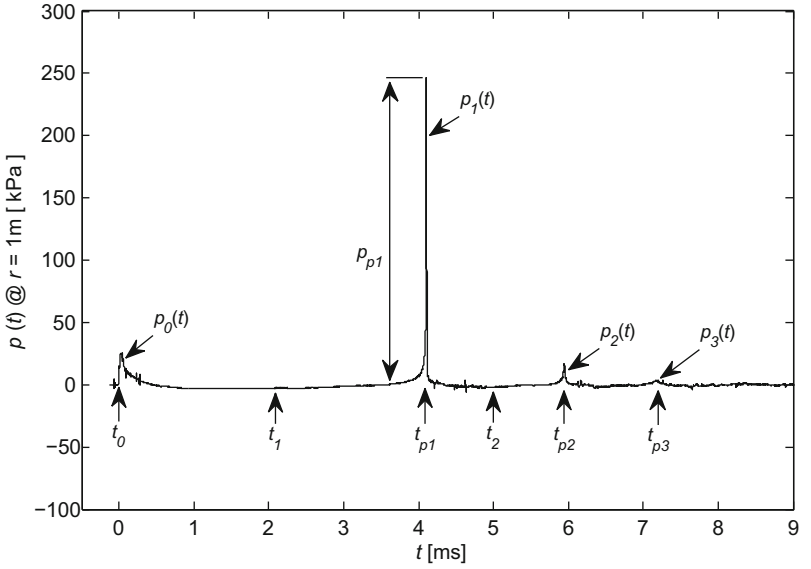

Fig. 6. An example of the measured acoustic pressure wave $p(t)$ (R_{M1}=24.5 mm, p_{zp1}=80.4, A_1=2.7868).

second maximum volume. The individual frames can be traced to corresponding points on the plot of bubble radius vs. time given in Fig. 8.

From the film records it was verified first of all that the bubbles generated in these experiments retained almost spherical shapes in the vicinity of the first and second maximum volumes. Though it is a relatively straightforward procedure to determine the bubble size (the maximum radius R_{M1}) from the film records, not much can be inferred about the bubble oscillation intensity from the frames. This question will be discussed in greater detail in Section 5. It could be also verified from the film records that the bubbles behave almost adiabatically during the first oscillation.

As already mentioned in this work great attention was paid to measuring the acoustic pressure waves radiated by oscillating bubbles. Recently, a total of several thousand pressure records have been obtained using different experimental configurations. An example of one pressure record is shown in Fig. 6. This pressure record has been measured at the distance r=0.1 m and recalculated to the nominal distance r=1 m.

As it can be seen in Fig. 6, the recorded wave consists of several pressure pulses, which can be identified as an initial pressure pulse $p_0(t)$, the first bubble pulse $p_1(t)$, the second bubble pulse $p_2(t)$, and so on.

The initial pressure pulse $p_0(t)$ is radiated during the delivery of energy into the discharge channel (bubble excitation phase). When the bubble attains its first maximum radius, R_{M1}, the maximum negative value in the acoustic pressure wave is radiated. When the bubble is compressed to a minimum radius, R_{m1}, the maximum positive value of the acoustic pressure wave is radiated. This maximum positive value is referred to as the peak pressure in the first bubble pulse, p_{p1}. The time interval between the time t_0, when the pressure in the initial pulse $p_0(t)$ starts rising, and an instant t_{p1}, when the pressure attains the peak value p_{p1}, corresponds to the time of the first bubble oscillation T_{o1}.

After the bubble is compressed to the first minimum radius R_{m1}, it starts a series of further oscillations during which it radiates the second bubble pulse $p_2(t)$, the third bubble pulse $p_3(t)$, etc.

In Section 2 we have already noticed that the peak pressure p_{p1} is very sensitive to the intensity of bubble oscillations. In the next section we shall use its non-dimensional form, as defined by Eq. (4), as a measure of the bubble oscillation intensity suitable for bubble description in experimental works.

4. The bubble map

The concept of what is here called the "bubble map" has been introduced in Ref. [3] to display the limits (frontiers) of different influences (such as liquid viscosity, heat conduction, gravity, etc.) on the bubble motion conveniently. The bubble map proved also very useful when comparing different experimental bubbles using only the two descriptive parameters, namely the bubble size and bubble oscillation intensity. In this case the bubble map is simply an X–Y scatter plot in which each point represents a single bubble.

As previously said, the bubble size of the spark generated bubbles can be easily determined from the pressure records. This was done by measuring the first oscillation period, T_{o1}, and assuming $T_{o1}=2T_{c1}$. Then Eq. (5) can be rearranged to yield

$$R_{M1} = \frac{T_{o1}}{2T_{zc1}\sqrt{\rho_\infty/p_\infty}}. \tag{6}$$

Please cite this article as: S. Buogo, & K. Vokurka, Intensity of oscillation of spark-generated bubbles, *Journal of Sound and Vibration* (2010), doi:10.1016/j.jsv.2010.04.030

In the case of scaling bubbles the non-dimensional compression time, T_{zc1}, is independent of the bubble size, R_{M1}. However, as it can be seen in Fig. 3, it depends on bubble oscillation intensity, p_{zp1}, and as follows from Eq. (4), the non-dimensional peak pressure, p_{zp1}, depends on the bubble size, R_{M1}. Thus we need to find R_{M1} and p_{zp1} from experimental values of r, T_{o1}, and p_{p1}, and from variation of T_{zc1} with p_{zp1}, as given in Fig. 3. A following iterative procedure has been used to solve this task.

For each pressure record we begin computations using a value of $T_{zc1}=0.93722$, which corresponds to $p_{zp1}=70$ in Fig. 3. This value represents a first estimate of T_{zc1}. Then using this value of T_{zc1} and a value of T_{o1} determined from a given pressure record, we compute from Eq. (6) the first estimate of R_{M1}. This estimate is then inserted together with corresponding values of p_{p1} and r into Eq. (4) to obtain a first estimate of p_{zp1}. Using this first estimate of p_{zp1} we can determine a second estimate of T_{zc1} from Fig. 3. With this second estimate of T_{zc1} we can calculate a second estimate of R_{M1} from Eq. (6) and a second estimate of p_{zp1} from Eq. (4). This procedure can be then repeated to obtain the third estimate of R_{M1} and p_{zp1}, and so on. Using theoretical data (in which case we know R_{M1} and p_{zp1} exactly) we have verified that satisfactory results can be obtained after only two iterations (i.e., after computing the third estimates of R_{M1} and p_{zp1}). A suitable code has been written in Matlab and all experimental records have been processed using this procedure. The values of R_{M1} and p_{zp1} obtained in this way for a selected experimental configuration are displayed in the bubble map shown in Fig. 7. The experimental configuration corresponds to charging voltage 4 kV and hydrophone TC4038.

The variation of T_{zc1} with p_{zp1} used in the iterative procedure (Fig. 3) has been determined with a theoretical model. It is evident that the reliability of the suggested iterative method will increase when this variation of T_{zc1} with p_{zp1} is determined experimentally, using, e.g., combination of a suitable optical method and pressure record measurements.

From the bubble map it can be seen that in the selected experiments a relatively broad range of both bubble sizes (R_{M1} ranging from 12.8 to 56.4 mm) and bubble oscillation intensities (p_{zp1} ranging from 14.3 to 174, which corresponds to A_1 ranging from 2.04 to 3.4, and to P^*_{m1} ranging from 0.01 to 0.069) was obtained.

It has been verified (e.g., by comparing the energy spectral densities of the records measured with the two hydrophones), that the points lying in the right lower corner of the bubble map have been recorded with high accuracy. On the other hand, uncertainty of the obtained peak pressure values is the highest at the left upper corner of the bubble map, where the limited bandwidth of the hydrophone may cause some filtering and thus the actual peak pressure might be higher than the measured one. However, even here the error does not seem to be extremely large. We intend to touch this point in greater detail in a separate work.

It should be noted here that a slightly different procedure is often used in literature to determine the bubble size from T_{o1} (see, e.g., Ref. [5]). That procedure is based on the so-called collapse time of an empty bubble $T_{zc1}=0.91468$, that was first analytically determined by Rayleigh [6]. We consider the procedure used here to be more appropriate for several reasons. First, Rayleigh has computed his collapse time under an assumption of an empty bubble (i.e., for $P^*_{m1}=0$, and as it

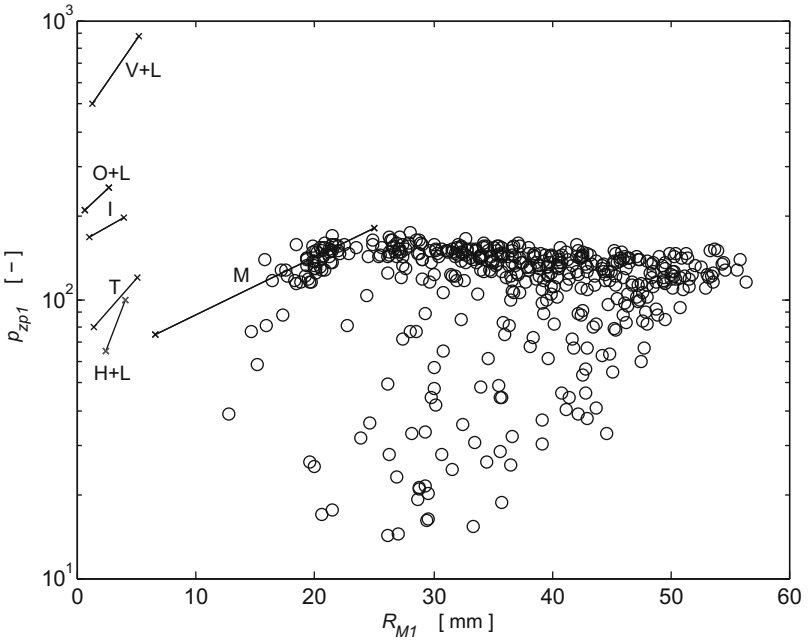

Fig. 7. The bubble map for the spark and laser generated bubbles. The non-dimensional peak pressure in the first bubble pulse p_{zp1} represents a measure of the bubble oscillation intensity; the first bubble maximum radius R_{M1} represents the bubble size. Each point (o) represents one experimental bubble. M – data from Mellen [7], T – data from Teslenko [8], H+L – data from Hentschel and Lauterborn [9], I – data from Isselin et al. [10], O+L – data from O. Lindau and Lauterborn [11], and V+L – data from Vogel and Lauterborn [12].

Please cite this article as: S. Buogo, & K. Vokurka, Intensity of oscillation of spark-generated bubbles, *Journal of Sound and Vibration* (2010), doi:10.1016/j.jsv.2010.04.030

Table 1
Comparison of the values of R_{M1} and p_{zp1} computed from the experimental data using, first, the Rayleigh's collapse time $T_{zc1}=0.91468$, and second, the iterative procedure described in this work.

	Experimental data	Rayleigh's result	Iterative procedure	Difference (%)
1st bubble	$r=0.1$ m, $p_{p1}=0.6235$ MPa $T_{o1}=4.6211$ ms	$R_{M1}=28.23$ mm $p_{zp1}=17.67$	$R_{M1}=26.51$ mm $p_{zp1}=18.81$	6.1 6.1
2nd bubble	$r=0.1$ m, $p_{p1}=4.1944$ MPa $T_{o1}=3.8520$ ms	$R_{M1}=23.53$ mm $p_{zp1}=142.60$	$R_{M1}=23.25$ mm $p_{zp1}=144.33$	1.2 1.2

can be seen from Eq. (1), this corresponds to infinite amplitude of the first bubble oscillation, i.e., to $A_1\to\infty$). Second, Rayleigh has assumed a non-compressible liquid. It is clear that real bubbles oscillate with finite amplitudes (see Fig. 7) and in compressible liquids. It must also be noted that the difference between the values of R_{M1} obtained with Rayleigh's collapse time T_{zc1} and using the iterative procedure introduced here is larger for small intensities of oscillation. As the intensity of oscillation increases, this difference keeps decreasing.

Let us give a concrete example considering two experimental pressure records. One has been obtained observing a bubble oscillating with low intensity and the other with high intensity. The experimental data determined from the two pressure records and the values of R_{M1} and p_{zp1} determined from Eqs. (4) and (6) using both the Rayleigh's collapse time $T_{zc1}=0.91468$, and the iterative procedure described here are summarized in Table 1.

As it could be expected, the difference between the two procedures is larger for the bubble oscillating with a low intensity than for the bubble oscillating with a high intensity. The reason for this can be seen in Fig. 3, where the compression time is approaching the Rayleigh's collapse time for larger oscillation intensities.

It is also interesting to compare the values found here and displayed in Fig. 7 with results of other authors. For example, Mellen [7] also studied spark generated bubbles. In his work the bubble sizes R_{M1} ranged from 6.5 to 25 mm and the non-dimensional peak pressures p_{zp1} ranged from 75 to 180. Teslenko [8] generated bubbles with a laser. In his experiments the bubble sizes R_{M1} ranged from 1.3 to 5 mm and the non-dimensional peak pressures p_{zp1} ranged from 80 to 120. Similarly, Hentschel and Lauterborn [9] report results obtained in experiments with laser generated bubbles. Their bubbles had sizes R_{M1} ranging from 2.3 to 4 mm and the measured non-dimensional peak pressures p_{zp1} ranged from 65 to 100. Isselin et al. [10] also generated bubbles by laser and in this case the bubble sizes R_{M1} ranged from 0.9 to 3.8 mm and the non-dimensional peak pressures p_{zp1} ranged from 167 to 197. Recently, Lindau and Lauterborn [11] published results of their measurement. Using their data one can see that in this case the bubble sizes R_{M1} ranged from 0.6 to 2.6 mm and the non-dimensional peak pressures p_{zp1} ranged from 210 to 250. Finally, in an earlier work Vogel and Lauterborn reported their results [12] obtained with bubbles generated by laser. According to data published in this case the bubble sizes R_{M1} ranged from 1.2 to 5.1 mm and the non-dimensional peak pressures p_{zp1} ranged from 500 to 880. As this last value is extremely high we prefer giving its computation here in detail. According to Fig. 10 in Ref. [12], for a bubble having a maximum radius $R_{M1}=5$ mm the measured peak pressure at a distance $r=10$ mm was $p_{p1}=440$ bar, then assuming $p_\infty=1$ bar, the non-dimensional peak pressure is $p_{zp1}=880$, as given above. The data of other authors are compared with results found in this work in Fig. 7.

All the values discussed in the previous paragraph were taken from graphs published in the respective works and the data have been recalculated to obtain the quantities used here. This procedure is certainly not very precise and thus the values given should be taken as illustrative first of all. Nevertheless, it can be seen that as far as the intensities of oscillations are concerned they are basically the same as found here or partially higher. All reported intensities are also increasing with the bubble size. It certainly would be interesting to know why are the bubbles oscillating more intensively in some experiments than in others and what is the cause for the increase of intensities with the bubble size. We intend to give a partial answer to these questions elsewhere. However, to obtain a deeper explanation, new experiments should be made aiming at explaining these questions.

5. Comparison of theoretical and experimental data

In this section, the experimental records will be compared with theoretical data obtained using the bubble model given in the Appendix. For this comparison an experimental bubble has been selected for which we have both a pressure record and a film record available and which is oscillating with a relatively low intensity so that no finite-amplitude wave effects in propagation of the radiated pressure wave have been observed.

Using the procedure described in Section 4, the bubble size, R_{M1}, and the non-dimensional peak pressure, p_{zp1}, of this bubble have been determined first. Then from Fig. 2 it was possible to determine the corresponding amplitude of the first bubble oscillations, A_1. After inserting this values of A_1 into the bubble model given in the Appendix it was possible to compute the theoretical variations of $R(t)$ and $p(t)$. These theoretical variations can be then compared with experimental records.

Please cite this article as: S. Buogo, & K. Vokurka, Intensity of oscillation of spark-generated bubbles, *Journal of Sound and Vibration* (2010), doi:10.1016/j.jsv.2010.04.030

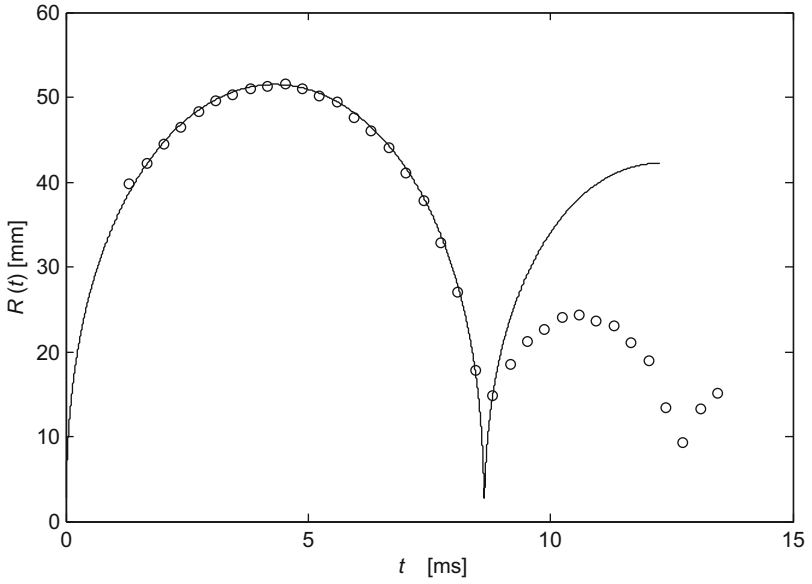

Fig. 8. Comparison of experimental (○) and theoretical (—) time histories of the bubble radius $R(t)$ (R_{M1}=51.5 mm, p_{zp1}=70.3, A_1=2.7156).

The variations of the bubble radius R with time t, both experimental and theoretical, are shown in Fig. 8.

The experimental points in Fig. 8 have been determined from frames as are those shown in Fig. 5. As the experimental bubble is not ideally spherical (it is slightly elongated in vertical direction), the data points represent an average from two perpendicular dimensions—one in a horizontal and the other in a vertical direction.

The origin of the time scale for experimental data can be determined from the film records only with an uncertainty equal to the time step between two subsequent frames and this time step is relatively large in the case of low framing rates (357 μs in this particular case). Hence the experimental points have been shifted along the time scale until the best agreement with a theoretical curve is obtained.

The theoretical curve has been computed for A_1=2.7156 starting at R_{M1} and ending at R_{M2}. The part of $R(t)$ between R_{M1} and R_{m1} has been then reverted and inserted into the figure to obtain the theoretical variation even for earlier times $t < t_1$. In doing this we have assumed that the time behavior of radius is symmetric around the time corresponding to the maximum radius R_{M1}. Times of different frames given earlier in Fig. 5 have been then taken from Fig. 8.

As it can be seen in Fig. 8, the theoretical curve fits the experimental points in the vicinity of R_{M1} relatively well. This is not surprising. It is well known that near R_{M1} the radius vs. time variation $R(t)$, when suitably matched to R_{M1}, is almost identical for all bubbles oscillating with sufficiently high intensities (cf. normalized radius vs. time variations corresponding to $A_1 > 2$ in Fig. II-1 in [13]). In other words, this "inverted tea cup" form is insensitive to the oscillation intensity. For different oscillation intensities the bubble radius vs. time will differ only in the vicinity of the bubble minimum radii, R_{m1}. As it can be seen in Fig. 8, this is a very narrow region lasting very shortly. The framing rate in the present experiment (2800 frames/s) was certainly not sufficient to examine this area in detail. However, as it is discussed elsewhere, even for the relatively large bubbles generated in these experiments, which are oscillating slowly (for the scaling bubbles the time of the first oscillation T_{o1} is directly proportional to the first bubble maximum radius R_{M1}—cf. Eq. (6)), the framing rate necessary to catch the details of the bubble motion near its minimum radius R_{m1} should be higher than 10^6 frames/s. When taking into account certain randomness always present in generating the experimental spark bubbles, the film record should be rather long. These requirements are still prohibitive for most experimental laboratories at present time. Thus, it is very difficult to estimate the bubble oscillation intensity from the film records, at least in our case. Therefore, it is also almost impossible to say anything about the actual value of R_{m1}.

As it can be seen in Fig. 8, the difference between theory and experimental points starts to grow for times $t > t_{p1}$ significantly. This is because the theoretical model used here assumes the so-called *gas* bubble. However, the experimental spark bubbles behave, most probably, at least for times $t > t_{p1}$, as the so-called *vapor* bubbles. Secondly, there might also be energy losses not taken into account in this theoretical model. These are very delicate topics that we wish to discuss in a separate work. Preliminary results in this respect have been given in Refs. [14,15].

An experimental pressure record is compared with a theoretical variation in Fig. 9. Both the experimental and theoretical pressure records correspond to the radius vs. time histories displayed in Fig. 8. A detailed view at Fig. 9 will reveal that there are no finite-amplitude waves effects present in the pressure record.

A certain agreement between the experimental pressure wave and theoretical pressure variation can be seen. However, as can be also seen, the theoretical bubble pulse is broader, and this is true especially for the trailing edge of the bubble

Please cite this article as: S. Buogo, & K. Vokurka, Intensity of oscillation of spark-generated bubbles, *Journal of Sound and Vibration* (2010), doi:10.1016/j.jsv.2010.04.030

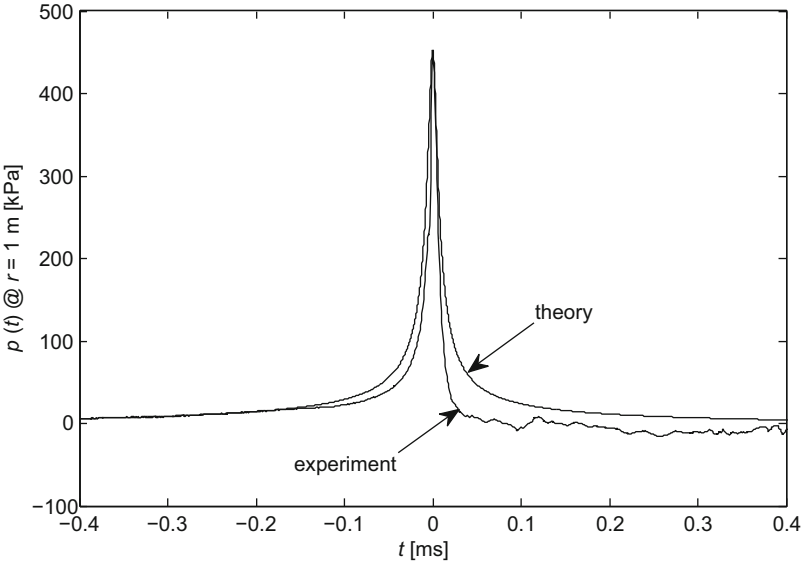

Fig. 9. Comparison of experimental and theoretical time plots of the acoustic pressures $p(t)$ in the first bubble pulse (R_{M1}=51.5 mm, p_{zp1}=70.3, A_1=2.7156). Only a small portion from the whole bubble pulse close to p_{p1} is displayed.

pulse. This point has been already briefly discussed elsewhere [15] and reference to it will be done once again later on in a separate work. Again this discrepancy only shows the differences between the experimental data and the present theory.

In discussing results displayed in Figs. 8 and 9 an important question arises on how to fit theoretical data to experimental data with best accuracy. In this work, a procedure based on fitting the peak pressure in the first bubble pulse p_{p1} and the first bubble maximum radius R_{M1} was used. Thus, we obtained a relatively good agreement between experimental data and theoretical curves both for the radius and acoustic pressures histories within the first time of bubble oscillation. However, for later times the theoretical variations start to depart from experimental data significantly. This departure is attributed here to an unsuitable theoretical bubble model, which is not taking into account all energy losses associated with bubble oscillations.

However, let us say here that a different approach is most often found in the literature (see, e.g., Refs. [5,18–24]). In that approach an agreement between experimental data and theoretical curves is sought just for the radius vs. time variation, and not only for the first time of bubble oscillation like here, but also for the second time of bubble oscillation. This means, one is trying to fit the theoretical curve to two maximum bubble radii, R_{M1} and R_{M2}. To obtain the required decrease in the bubble radius R_{M2}, the bubble oscillation intensity in the theoretical model is increased up to a degree, when radiated acoustic energy covers all excessive energy losses in the experimental bubble, that is, until the computed second maximum radius, R_{M2}, agrees with the experimentally determined one. In this case one obtains a good fit of the radius vs. time history up to the second maximum radius R_{M2}. However, let us remark that in this case the calculated peak pressures in the first bubble pulse, p_{p1}, will exceed by far the measured peak pressures.

It is clear that this point will require further discussions and further supporting arguments, both experimental and theoretical ones, to decide which approach is more correct. Nevertheless, let us remind that earlier arguments supporting our assumptions can be found in Ref. [3]. These earlier arguments have been based on experimental data published in literature. Now using our own experimental data we intend to discuss this point in greater detail in a separate publication.

6. Conclusions

In the present work it is suggested that to describe adequately a spherical bubble oscillating in a liquid in a zero-order mode (pulsating bubble), beside knowing the liquid and gas properties and the ambient pressure and temperature, at least two further parameters are needed: the bubble size and bubble oscillation intensity. The first maximum bubble radius, R_{M1}, can conveniently describe the bubble size. The bubble oscillation intensity can be described in theoretical works by the amplitude of the first oscillation, A_1, and in experimental works by the non-dimensional peak pressure in the first bubble pulse, p_{zp1}.

An iterative procedure suitable to determine both R_{M1} and p_{zp1} from pressure waves, radiated by oscillating bubbles, was introduced. The procedure is demonstrated on a set of acoustic pressure waves recorded in recent experiments with spark generated bubbles. The calculated values of these two parameters are displayed in the bubble map. It can be seen that in the present experiments the bubble sizes R_{M1} ranged from 12.8 to 56.4 mm, and the bubble intensities, p_{zp1}, from 14.3 to 174.

Please cite this article as: S. Buogo, & K. Vokurka, Intensity of oscillation of spark-generated bubbles, *Journal of Sound and Vibration* (2010), doi:10.1016/j.jsv.2010.04.030

To keep the discussion within reasonable limits many points have been assumed but not discussed here. These points concern, for example, reliability of the measured pressure records. To measure p_{p1} correctly the recording apparatus must have a suitable bandwidth. Preliminary results concerning this question have been published at a seminar [16]. Another important point concerns assumption of the scaling bubbles. Also in this case the discussion of this question is postponed to elsewhere. It was also assumed that no shock fronts develop in the first bubble pulse during its propagation in the liquid. Preliminary results concerning the limits for the finite amplitude wave propagation effects have been presented at a seminar [17] and it has been shown that the limiting intensity of bubble oscillations is approximately $p_{zp1}=80$. For lower intensities of bubble oscillations no nonlinear effects in pressure wave propagation have been observed. Exactly these weakly oscillating bubbles have been used here to demonstrate some important points.

The intensity of bubble oscillation has been introduced here because it is believed to be an important parameter for describing the oscillating bubbles. However, it should be also said here that it is not common in the literature to use any explicitly defined intensity measure though the intensity measure is always present in computations, if not explicitly, then implicitly, e.g., in a form of initial conditions, in a form of the driving pressure field, etc. To prove that it is not a superfluous parameter, we intend to exploit this new intensity concept also in other contexts, e.g., when determining experimental scaling functions or spectral properties of the bubble pulses. As already mentioned it has been used recently to find a suitable hydrophone's bandwidth [16] and to determine conditions under which the shock fronts may develop in bubble pulses [17]. On the other hand it is difficult to predict whether the intensity measure suggested here (p_{zp1}) could be successfully used in a more complex environment, such as that encountered in clinical situations [26]. Only new experiments can verify this issue.

Acknowledgement

This work has been partly (K.V.) supported by the Ministry of Education of the Czech Republic as the research project MSM 467 478 8501.

Appendix. A theoretical model

In the following, equations defining Herring's simplified model will be given. This model has been selected because, in our experience [15], it gives the best fit to experimental data. However, as we have pointed out several times in the text, the overall accuracy of the model is not satisfactory. Let us say here that the accuracy would be not increased by using a different liquid compressibility equation (e.g., Gilmore's equation). In our opinion the problem lies in the fact that we do not know all the processes associated with the bubble oscillations satisfactorily at present time and this gap in our knowledge cannot be overcome by theoretical speculations, but only by collecting the experimental evidence first.

In Herring's simplified model of the scaling bubble the equation of motion for the bubble wall has a form [25]

$$\ddot{R}R+\frac{3}{2}\dot{R}=\frac{1}{\rho_\infty}\left(P-p_\infty+P\frac{\dot{R}}{c_\infty}\right). \tag{A.1}$$

Here R denotes the bubble radius, ρ_∞ the liquid density, P the pressure in the liquid at the bubble wall, p_∞ the ambient pressure and c_∞ the speed of sound in the liquid. Dots denote differentiating with respect to time. For the tasks solved here the initial conditions of Eq. (A.1) are $R(0)=R_{M1}$ and $\mathrm{d}R(0)/\mathrm{d}t=0$.

For the scaling bubbles the gas inside the bubble is assumed to be compressed and expanding adiabatically and the effects of surface tension, liquid viscosity and gravity need not be considered. Then the pressure in the liquid at the bubble wall can be written as

$$P=p_\infty\left(\frac{R}{R_0}\right)^{-3\gamma}. \tag{A.2}$$

Here γ is the ratio of specific heats.

For moderate bubble oscillation intensities, for which no finite-amplitude wave effects can be expected, the acoustic wave $p(t)$ radiated by the bubble can be conveniently determined using a simple expression

$$p=p_t-p_\infty=\left(P-p_\infty+\frac{1}{2}\rho_\infty\dot{R}^2\right)\frac{R}{r}. \tag{A.3}$$

Here p_t is the total pressure field in the liquid and r is the point in the liquid in which $p(t)$ is being determined.

With respect to experiments reported in this work the maximum radii of the theoretical bubbles shown in Figs. 1a and b have been selected to be in the range from 25 to 40 mm (equilibrium radius $R_0=20$ mm) and Eqs. (A.1)–(A.3) have been solved using the following values of the environmental and physical quantities:

$$p_\infty=127.5\,\mathrm{kPa}\quad \rho_\infty=10^3\,\mathrm{kg\,m^{-3}},\quad c_\infty=1480\,\mathrm{m\,s^{-1}},\quad \gamma=1.25.$$

For the given amplitude A_1 the initial pressure at the bubble wall, P_{m1}, has been determined using Eqs. (1) and (3).

Please cite this article as: S. Buogo, & K. Vokurka, Intensity of oscillation of spark-generated bubbles, *Journal of Sound and Vibration* (2010), doi:10.1016/j.jsv.2010.04.030

The theoretical model presented above assumes adiabatic bubbles, for which thermal losses are not important. However, readers studying smaller bubbles and thus interested in incorporating thermal losses into a theoretical model can find suitable treatments, for example, in Refs. [27–29]. The case where the bubbles lose their sphericity can be dealt with using an approach presented in [30].

References

[1] T.G. Leighton, *The Acoustic Bubble*, Academic Press, London, 1994 (Chapter 5.4).
[2] F.R. Young, *Cavitation*, Imperial College Press, London, 1999 (Chapters 4.13 and 8).
[3] K. Vokurka, Amplitudes of free bubble oscillations in liquids, *Journal of Sound and Vibration* 141 (1990) 259–275.
[4] R.J. Bobber, *Underwater Electroacoustic Measurements*, Peninsula, Los Altos, CA, 1988 (Chapter 1.7).
[5] W. Lauterborn, T. Kurz, R. Mettin, C.D. Ohl, Experimental and theoretical bubble dynamics, *Advances in Chemical Physics* 110 (1999) 295–379.
[6] Lord Rayleigh, On the pressure developed in a liquid during the collapse of a spherical cavity, *Philosophical Magazine* 34 (1917) 94–98.
[7] R.H. Mellen, An experimental study of the collapse of a spherical cavity in water, *Journal of the Acoustical Society of America* 28 (1956) 447–454.
[8] V.S. Teslenko, Experimental investigation of kinetic-electrical features of collapsing bubble from laser breakdown in viscous liquids, *Zhurnal Prikladnoi Mekhaniki i Tekhniceskoi Fyziki* 4 (1976) 109–117 (in Russian).
[9] W. Hentschel, W. Lauterborn, Acoustic emission of single laser-produced cavitation bubbles and their dynamics, *Applied Scientific Research* 38 (1982) 225–230.
[10] J.-C. Isselin, A.-P. Alloncle, M. Autric, On laser induced single bubble near a solid boundary: contribution to the understanding of erosion phenomena, *Journal of Applied Physics* 84 (1998) 5766–5771.
[11] O. Lindau, W. Lauterborn, Laser-produced cavitation—studied with 100 million frames per second, *Proceedings of the Fifteenth International Symposium on Nonlinear Acoustics*, Gottingen, September 1999, pp. 385–388.
[12] A. Vogel, W. Lauterborn, Acoustic transients generation by laser-produced cavitation bubbles near solid boundaries, *Journal of the Acoustical Society of America* 84 (1988) 719–731.
[13] K. Vokurka, On Reyleigh' s model of a freely oscillating bubble. II. Results, *Czechoslovak Journal of Physics* B35 (1985) 110–120.
[14] S. Buogo, J. Plocek, K. Vokurka, Efficiency of energy conversion in underwater spark discharges and associated bubble oscillations: experimental results, *Acta Acustica united with Acustica* 95 (2009) 46–59.
[15] K. Vokurka, S. Buogo, Acoustical approach to analysis of energy conversions in an oscillating bubble, *Proceedings of the Seventy-ninth Acoustic Seminar*, Malá Morávka, Czech Republic, October 2009, pp. 25–32. Available also at 〈http://www.kfy.tul.cz/vokurka.html〉.
[16] K. Vokurka, S. Buogo, A minimum hydrophone bandwidth for undistorted cavitation noise measurement, *Proceedings of the Seventy-sixth Acoustic Seminar*, Hodonín, Czech Republic, May 2008, pp. 99–108. Available also at 〈http://www.kfy.tul.cz/vokurka.html〉.
[17] K. Vokurka, S. Buogo, Experimental study of strong pressure pulses radiated by oscillating spark bubbles, *Proceedings of the Seventy-eighth Acoustic Seminar*, Železná Ruda, Czech Republic, May 2009, pp. 25–34. Available also at 〈http://www.kfy.tul.cz/vokurka.html〉.
[18] K.J. Ebeling, The behavior of spherical, laser-produced cavitation bubbles in water, *Acustica* 40 (1978) 229–239 (in German).
[19] B.P. Barber, S.J. Putterman, Light scattering measurements of repetitive supersonic implosion of a sonoluminescing bubble, *Physical Review Letters* 69 (1992) 3839–3842.
[20] R. Lofstedt, K. Weninger, S. Putterman, B.P. Barber, Sonoluminescing bubbles and mass diffusion, *Physical Review E* 51 (1995) 4400–4410.
[21] C.-D. Ohl, A. Philipp, W. Lauterborn, Cavitation bubble collapse studied at 20 million frames per second, *Annalen der Physik* 4 (1995) 26–34.
[22] C.-D. Ohl, T. Kurz, R. Geisler, O. Lindau, W. Lauterborn, Bubble dynamics, shock waves and sonoluminescence, *Philosophical Transactions of the Royal Society of London Series A* 357 (1999) 269–294.
[23] M. Muller, W. Garen, S. Koch, F. Marsik, W. Neu, E. Saburov, Shock waves and cavitation bubbles in water and isooctane generated by Nd:YAG laser, Experimental and theoretical results, *Proceedings of the Tenth International Conference on Laser-Assisted Micro- and Nanotechnologies*, St. Petersburg, June–July 2003, pp. 275–282.
[24] T. Kurz, D. Kroninger, R. Geisler, W. Lauterborn, Optic cavitation in an ultrasonic field, *Physical Review E* 74 (2006) 066307.
[25] K. Vokurka, Comparison of Rayleigh's, Herring's, and Gilmore's models of gas bubbles, *Acustica* 59 (1986) 214–219.
[26] T.G. Leighton, F. Fedele, A.J. Coleman, C. McCarthy, S. Ryves, A.M. Hurrell, A. De Stefano, P.R. White, A passive acoustic device for real-time monitoring of the efficacy of shockwave lithotripsy treatment, *Ultrasound in Medicine and Biology* 34 (2008) 1651–1665.
[27] R.I. Nigmatulin, N.S. Khabeev, F.B. Nagiev, Dynamics, heat and mass transfer of vapour-gas bubbles in a liquid, *International Journal of Heat and Mass Transfer* 24 (1981) 1033–1044.
[28] A. Prosperetti, L.A. Crum, K.W. Commander, Nonlinear bubble dynamics, *Journal of the Acoustical Society of America* 83 (1988) 502–514.
[29] T.G. Leighton, S.D. Meers, P.R. White, Propagation through nonlinear time-dependent bubble clouds and the estimation of bubble populations from measured acoustic characteristics, *Proceedings of the Royal Society of London Series A* 460 (2004) 2521–2550.
[30] C.K. Turangan, A.R. Jamaluddin, G.J. Ball, T.G. Leighton, Free-Lagrange simulations of the expansion and jetting collapse of air bubbles in water, *Journal of Fluid Mechanics* 598 (2008) 1–25.

Please cite this article as: S. Buogo, & K. Vokurka, Intensity of oscillation of spark-generated bubbles, *Journal of Sound and Vibration* (2010), doi:10.1016/j.jsv.2010.04.030